

*Article*

## Crystallization of Lead Phosphate in Gel Systems

Oratai Saisa-ard and Kenneth J. Haller\*

School of Chemistry, Institute of Science, Suranaree University of Technology, Nakhon Ratchasima 30000, Thailand

E-mail: ken.haller@gmail.com\*

**Abstract.** Lead phosphate crystals were grown in agarose gel at room temperature. Nucleation and crystal growth rates were controlled by changing the density of the gel medium including pure and phosphate gel. Individual crystallites from the pure gel layer show equant habit while those from the  $\text{PO}_4^{3-}$  gel layer show plate-like habit. Vibrational spectra indicate that the  $\text{PO}_4^{3-}$  ion is distorted and its symmetry is lower than free ion symmetry. Powder diffraction patterns of the pure gel products show mixed phases of  $\text{PbHPO}_4$ ,  $\text{Pb}_3(\text{PO}_4)_2$ , and  $\text{Pb}_5(\text{PO}_4)_3\text{OH}$  (PbHAp) consistent with saturation index predictions obtained from the PHREEQC program. Formation of the microscopic crystalline products was accompanied by a decrease in pH from 8 (theoretical for all layers mixed) to 3 for all reactions studied, consistent with  $\text{PbHPO}_4$  being the major product. PbHAp does not appear in the phosphate gel layer because of the higher Pb:P ratio required for the PbHAp phase relative to the  $\text{Pb}_3(\text{PO}_4)_2$  phase. PbHAp crystals from the gel crystallization method are first reported in this work as microcrystalline product deposited on the surface of the dominant phase formed in the pure gel layer.

**Keywords:** Lead phosphate, gel crystallization.

ENGINEERING JOURNAL Volume 16 Issue 3

Received 22 November 2011

Accepted 28 May 2012

Published 1 July 2012

Online at <http://www.engj.org/>

DOI:10.4186/ej.2012.16.3.161

*This paper is based on the poster presentation at the German-Thai Symposium on Nanoscience and Nanotechnology 2011—Green Nanotechnology of the Future, GTSNN 2011, in Nakhon Ratchasima, Thailand, 13-16 September 2011.*

## 1. Introduction

Crystallization in gels is attractive for study due to the simplicity of the technique and the effectiveness in growing single crystals with very high perfection that are difficult to grow by other techniques. It has been applied to the study of crystal formation in human-related system such as cholesterol stone, gall stones, and urinary calculi. Furthermore, it provides an ideal technique to study crystal deposition diseases, which could lead to better understanding of the cause of disease [1-3].

Lead phosphates are interesting materials due to their properties. Lead hydrogen phosphate ( $\text{PbHPO}_4$ ) and lead nitrate phosphate ( $\text{Pb}_2(\text{NO}_3)(\text{PO}_4)$ ) show dielectric, piezoelectric, and optical properties which are useful in transducers and memory devices. Trilead bis(phosphate) ( $\text{Pb}_3(\text{PO}_4)_2$ ) is known as a ferroelastic material with a phase transition near 180 °C [4-5]. While several researchers [6-9] have reported the growth of  $\text{PbHPO}_4$  and  $\text{Pb}_2(\text{NO}_3)(\text{PO}_4)$  in silica hydrogel, tetramethoxysilane gel, cross-linked polyacrylamide gel, agar gel, and gelatin, the appearance of small crystals of lead hydroxyapatite,  $\text{Pb}_5(\text{PO}_4)_3(\text{OH})$ , ( $\text{PbHAp}$ ), in the gel layers or on the surfaces of other lead phosphate products has not been reported.  $\text{PbHAp}$  is a material of biological interest because of the similarity to calcium hydroxyapatite,  $\text{Ca}_5(\text{PO}_4)_3(\text{OH})$ , ( $\text{CaHAp}$ ), the dominant component in mammalian hard tissues such as bones and teeth; about 69 wt% and 95 wt%, respectively [10]. The relationship of  $\text{PbHAp}$  to  $\text{CaHAp}$  and its link to bone diseases like osteoporosis make the crystallization and growth of these materials of interest.

This paper presents results of lead phosphate growth in agarose gel with varied density of the gel medium. The PHREEQC speciation program is first used in this work to calculate possible phases in the lead phosphate system supporting formation of  $\text{PbHAp}$  and other lead phosphate phases. The relationship between synthesis conditions and crystal phases of products, including the formation of  $\text{PbHAp}$ , are discussed based on the results obtained.

## 2. Experimental

### 2.1. Sample Preparation

Diffusion of two soluble compounds through the agarose gel was set for the crystal growth in tubes as illustrated schematically in Fig. 1. Crystalline products are obtained in the gel when the two reactants meet. Diammonium hydrogen phosphate,  $(\text{NH}_4)_2\text{HPO}_4$ , and lead(II) nitrate,  $\text{Pb}(\text{NO}_3)_2$ , were used as  $\text{PO}_4^{3-}$  and  $\text{Pb}^{2+}$  sources, respectively. Varied densities of phosphate gel (1.0, 1.3, 1.5, 1.7, and 2.0 % w/v of agarose) were prepared by dissolving agarose powder (Vivantis, molecular biology grade) in 20 mL DI water with stirring for 10 min at 100 °C to give clear solutions. Crystallization experiments were set in small test tubes (1.5 x 10 cm) by adding 3.0 mL of the appropriate hot gel solution to 2.5 mL of warm 0.6 M phosphate solution (Ajax Finechem, AR grade), adjusting pH to 10 with NaOH, and allowing the mixture to stand 20 min to cool to room temperature to gel. A second layer of pure gel (1.0, 1.5, and 2.0 % w/v) was created by adding 1.5 mL of pure gel solution on top of the  $\text{PO}_4^{3-}$  gel layer and allowing 20 min to set the pure gel layer, after which 2.5 mL of 1.0 M lead nitrate solution (Ajax Finechem, AR grade) at natural pH was added on top of the gel layers. All reactions were kept at room temperature for two weeks.  $\text{CO}_2$  was purged from the lead solution by passing Ar gas through the solution for 5 min before transfer.

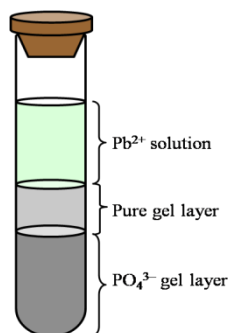


Fig. 1. Experimental set up for gel crystallization of lead phosphate phases.

After two weeks the remaining solution was removed and the gel layers separated. Each gel layer was warmed to melt the gel and the solid products filtered off. The three solutions were combined and pH measured. The solids were washed with cold DI water and dried at 100 °C for 24 h.

## 2.2. Characterization

Crystal morphologies were observed by optical microscopy using an Olympus SZ40 microscope (Olympus, Japan) and scanning electron microscopy (SEM) using a JSM 6400 electron microscope (JEOL, Japan). IR spectra were acquired on a Perkin-Elmer model Spectrum GX Fourier transform infrared spectrophotometer (FTIR) in wave number range 400-4000  $\text{cm}^{-1}$  from KBr pellets. Powder X-ray diffraction (XRD) scans were used for phase identification,  $2\theta$  range 10-60° using a Bruker axis D5005 diffractometer equipped with a  $\text{Cu K}\alpha$  X-ray source operating at 40 kV and 40 mA. The speciation program, PHREEQC V2 [11], with the *minteq.v4.dat* database [11] was used to calculate potential phase formation in the system assuming complete instantaneous mixing of the reactants.

## 3. Results and Discussion

Crystalline products were obtained inside both pure and  $\text{PO}_4^{3-}$  gel layers for all reactions as observed after two weeks reaction time. A typical result (density of phosphate and pure gel of 1.7 and 2.0 % w/v, respectively) is shown in Fig. 2.

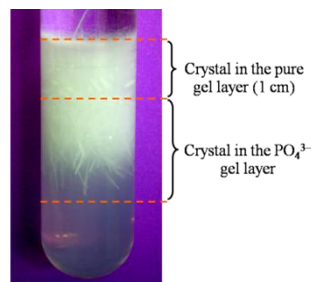


Fig. 2. Crystalline products in pure and  $\text{PO}_4^{3-}$  gel layers for a typical reaction (see text).

Microscopic crystalline products were accompanied by a decrease in pH to 3 for all reactions studied. Their morphologies as observed by optical microscopy and SEM are illustrated in Fig 3.

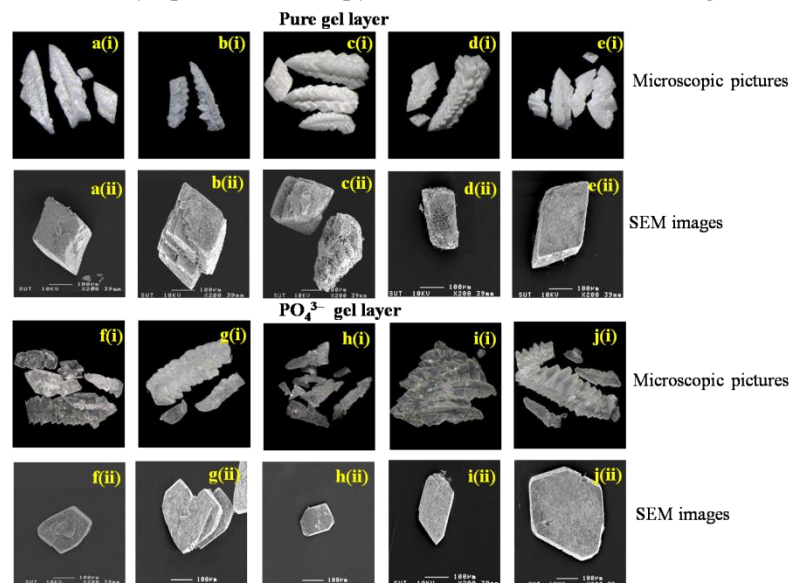


Fig. 3. Microscopic pictures (2.5X) (i) and SEM images (ii) of products formed in the pure gel layer: (a-e) and  $\text{PO}_4^{3-}$  gel layer (f-j) with 2.0 % w/v of pure gel but different density of phosphate gel: (a) 1.0, (b) 1.3, (c) 1.5, (d) 1.7, (e) 2.0 % w/v.

Products appear as aggregates under optical microscopy in the pure gel layer (Fig. 3a(i)-e(i)) and in the  $\text{PO}_4^{3-}$  gel layer (Fig. 3f(i)-j(i)). Individual crystallites from the pure gel layer show equant habit (Fig. 3a(ii)-e(ii)), and those from the  $\text{PO}_4^{3-}$  gel layer show plate-like habit (Fig. 3f(ii)-j(ii)) as seen in low magnification SEM images.

Needle-like crystals with dimension about  $2.5 \times 10 \mu\text{m}$  are deposited on the surfaces of crystal products formed in the pure gel layer as can be seen in SEM images at higher magnification as shown in Fig. 4. These crystals have similar morphology to that reported by Mavropoulos *et al.* [12] for PbHAp. This observation further confirms that multiple product phases occur in this system, and indicates that they occur in sequential fashion. These small crystallites observed only in the pure gel layer occur for all the different densities of  $\text{PO}_4^{3-}$  gel layer.

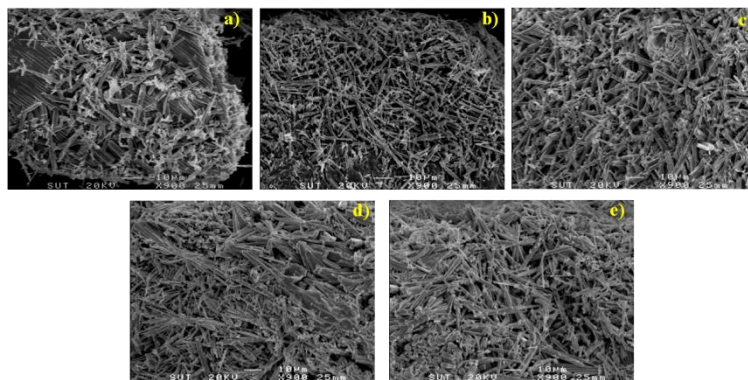


Fig. 4. SEM images of crystal products obtained in the pure gel layer (2.0 % w/v), formed with different densities of  $\text{PO}_4^{3-}$  gel: (a) 1.0, (b) 1.3, (c) 1.5, (d) 1.7, (e) 2.0 % w/v.

IR wave number and assignments for the products are given in Table 1. All products give almost identical spectra that show characteristic bands of  $\text{PO}_4^{3-}$  group; bands in the regions  $955\text{-}1046 \text{ cm}^{-1}$ ,  $923\text{-}924 \text{ cm}^{-1}$ , and  $519\text{-}601 \text{ cm}^{-1}$  reveal the asymmetric P–O stretching ( $\nu_3$ ), symmetric P–O stretching ( $\nu_1$ ), and O–P–O bending ( $\nu_4$ ), respectively.

Table 1. IR frequencies ( $\text{cm}^{-1}$ ) and assignments of crystal products from pure and phosphate gel layer.

Crystal in the pure gel layer	Crystal in the $\text{PO}_4^{3-}$ gel layer	Assignment
$\sim 3555$ w, b		$(\nu_1 + \nu_3)$ $\text{H}_2\text{O}$ stretch
$\sim 1604$ m		$\nu_2$ $\text{H}_2\text{O}$ bend
1384 vs	~1100 s,b	} $(\nu_1 + \nu_3)$ $\text{NO}_3$ , stretch
1348 vs		
1046 sh		
1004-1005 vs		
955-956 vs		
923-924 vs		$\nu_1$ $\text{PO}_4$ , $\nu_1$ $\text{HPO}_4$ stretch
813-814 vw		$\nu_2$ $\text{NO}_3$ bend
715-716 vw	}	} $\text{H}_2\text{O}$ libration
705-706 vw		
600-601 m	}	} $\nu_4$ $\text{PO}_4$ bend
539 m		
519-520 m		
398 sh	449 w	} $\nu_2$ $\text{PO}_4$ bend,
	388 vw	

Abbreviations: w = weak, m = medium, s = strong, v = very, sh = shoulder, b = broad.

Assignments:  $\nu_1$  = symmetric stretching,  $\nu_2$  = bending,  $\nu_3$  = asymmetric stretching,  $\nu_4$  = bending.

An ideal  $\text{PO}_4^{3-}$  anion has tetrahedral point symmetry. Only absorptions corresponding to the  $\nu_3$  (955-1046  $\text{cm}^{-1}$ ) and  $\nu_4$  (519-601  $\text{cm}^{-1}$ ) vibrations should be observed. The  $\nu_1$  (923-924  $\text{cm}^{-1}$ ) and  $\nu_2$  (388-449  $\text{cm}^{-1}$ ) vibrations would be allowed in lower symmetry groups. The appearance of  $\nu_1$  and  $\nu_2$  in the IR spectra of both products from pure and  $\text{PO}_4^{3-}$  gel layers indicates the lower symmetry of  $\text{PO}_4^{3-}$  in the structure [13-14]. Water bending mode (1604  $\text{cm}^{-1}$ ) and O–H stretching mode (3555  $\text{cm}^{-1}$ ) are observed for the products obtained inside the pure gel layer but not for products obtained inside the  $\text{PO}_4^{3-}$  gel layer.

Bands at 1348-1384 and 813-814  $\text{cm}^{-1}$  of products formed inside the pure gel layer which disappear after heating at 600 °C (Fig. 5) are assigned to residual nitrate from starting compound in agreement with previous work [15].

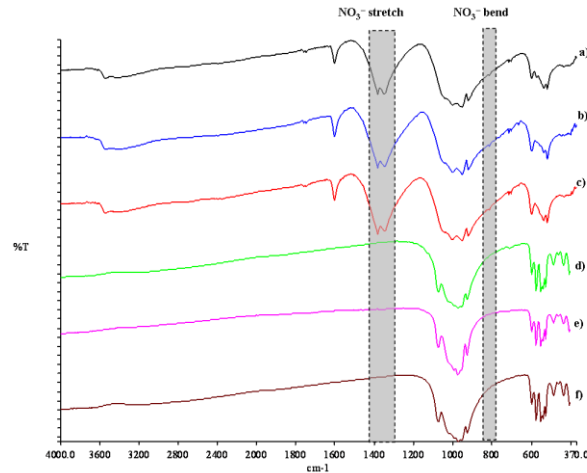


Fig. 5. IR spectra of products formed in the pure gel layer (2.0 % w/v) before heating; (a) 1.0, (b) 1.5, (c) 2.0 % w/v of  $\text{PO}_4^{3-}$  gel, and after heating at 600 °C; (d) 1.0, (e) 1.5, (f) 2.0 % w/v of  $\text{PO}_4^{3-}$  gel.

Search-match of the XRD patterns of crystal products obtained in the pure gel layer identify mixed phases containing PbHAp (JCPDS 1-0924),  $\text{PbHPO}_4$  (JCPDS 6-0274), and  $\text{Pb}_3(\text{PO}_4)_2$  (JCPDS 13-0278) as shown in Fig. 6(i) while products formed in the  $\text{PO}_4^{3-}$  gel layer show only peaks due to  $\text{PbHPO}_4$  and  $\text{Pb}_3(\text{PO}_4)_2$  (Fig. 6(ii)). Peaks due to PbHAp and  $\text{Pb}_3(\text{PO}_4)_2$  phases are difficult to see because they are minor products. Small needle-like PbHAp crystals on the surface of products separated from the pure gel layer can be seen in the SEM images in Fig. 4. These results are consistent with predictions (assuming instantaneous mixing of all reactants in an aqueous solution) obtained from the PHREEQC program that calculates saturation indices based on aqueous solution activities for all species involved.

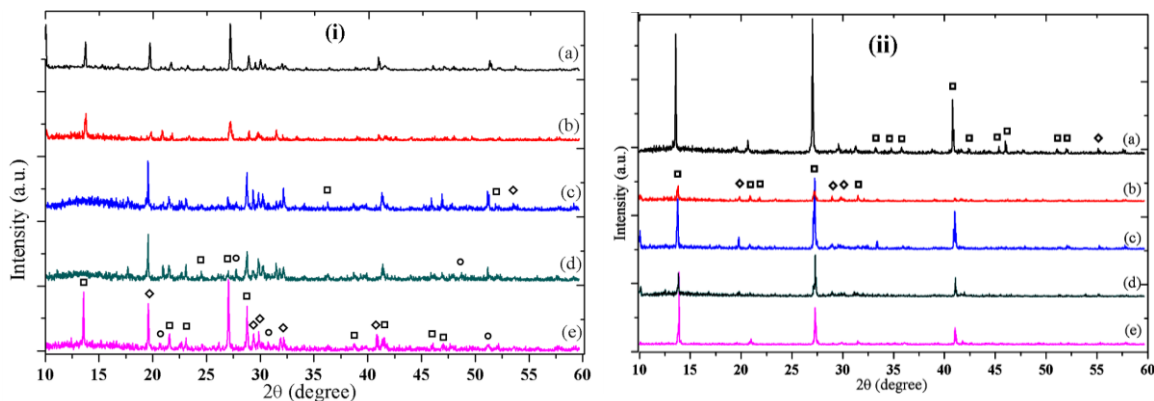


Fig. 6. XRD patterns of products obtained in the pure gel layer (i) and phosphate gel layer (ii) formed with 2.0 % w/v of pure gel and different densities of the phosphate gel: (a) 1.0, (b) 1.3, (c) 1.5, (d) 1.7, (e) 2.0 % w/v; (□)  $\text{PbHPO}_4$ , (◇)  $\text{Pb}_3(\text{PO}_4)_2$ , (○) PbHAp.

Saturation index (SI) uses calculated activities to provide a good indicator of the potential solid phases in a system at its equilibrium state [16]. SI is defined as Eq. (1):

$$SI = \log \left( \frac{IAP}{K_{sp}} \right) \quad (1)$$

where IAP is the free ionic activity product and  $K_{sp}$  is the thermodynamic solubility product constant of a pure precipitate phase. SI relates to  $\Delta G$  [17] as,

$$\Delta G = -2.303RT \log \left( \frac{IAP}{K_{sp}} \right) \quad (2)$$

where  $R$  is the ideal gas constant, and  $T$  is the temperature. From Eq. (2),  $\Delta G$  equals zero when  $IAP = K_{sp}$  corresponding to  $SI = 0$  and the solution is in equilibrium;  $\Delta G$  is negative when  $IAP > K_{sp}$  corresponding to  $SI > 0$ ; the solution is supersaturated and precipitation can occur (unless a metastable supersaturated solution occurs). However,  $\Delta G$  is positive when  $IAP < K_{sp}$  corresponding to  $SI < 0$  and the solution is undersaturated so precipitation cannot occur.

Calculation of SI requires detailed knowledge of the speciation of phosphate, lead compounds, and other related ions in the system. Speciation of relevant phosphate and lead compounds in the system is given in Table 2.

Table 2. Stability constants ( $K_a$ ) for  $H_3PO_4$  speciation, and solubility constants ( $K_{sp}$ ) and saturation index (SI) for various lead compounds.

<b><math>H_3PO_4</math> speciation</b>		<b><math>pK_a^a</math></b>	
$H_3PO_4 \rightleftharpoons H_2PO_4^- + H^+$		2.20	
$H_2PO_4^- \rightleftharpoons HPO_4^{2-} + H^+$		7.17	
$HPO_4^{2-} \rightleftharpoons PO_4^{3-} + H^+$		12.35	
<b>Relevant lead compounds</b>		<b><math>pK_{sp}^b</math></b>	<b>SI<sup>c</sup></b>
$Pb_5(PO_4)_3OH + 7H^+ \rightleftharpoons 5Pb^{2+} + 3H_2PO_4^- + H_2O$		62.79	13.17
$Pb_3(PO_4)_2 + 4H^+ \rightleftharpoons 3Pb^{2+} + 2H_2PO_4^-$		43.53	7.88
$PbHPO_4 \rightleftharpoons Pb^{2+} + HPO_4^{2-}$		23.80	2.08
$Pb(OH)_2 + 2H^+ \rightleftharpoons Pb^{2+} + 2H_2O$		-8.18	-0.48

<sup>a</sup> Values from reference [16].

<sup>b</sup> Values from *minteq.v4.dat* database in reference [11].

<sup>c</sup> This work for the system described in the text.

An initial pH = 10 in the  $PO_4^{3-}$  gel and initial pH of 6 in the 1M  $Pb(NO_3)_2$  solution, imply a pH gradient through the “pure” gel layer from 10 to 6 as the reactants diffuse together (if all three layers were instantaneously mixed as an aqueous solution the pH would be 8). At pH = 10 the phosphate speciation (Fig. 7) predicts a small  $PO_4^{3-}$  concentration and  $HPO_4^{2-}$  as the dominant species. At pH = 6  $H_2PO_4^-$  is the dominant species with only a few percent  $HPO_4^{2-}$  and even less  $PO_4^{3-}$ . PHREEQC calculations based on the total initial concentrations of species in all layers combined indicate that  $PbHPO_4$ ,  $Pb_3(PO_4)_2$ , and  $PbHAp$  would be supersaturated (pH = 8, and SI = 2.08, 7.88, and 13.17, respectively). The larger SI for the  $PO_4^{3-}$  containing species in spite of the low  $PO_4^{3-}$  concentration is a result of their solubilities being considerably lower than that of the  $HPO_4^{2-}$  containing species, and suggests they may nucleate first.

As phosphate ion is removed from the gel by precipitation, the speciation equilibrium will convert  $HPO_4^{2-}$  to  $H^+$  and  $PO_4^{3-}$ , lowering the pH and at the same time adjusting the relative ion concentrations to favor  $HPO_4^{2-}$  until the hydrogen phosphate species nucleates. Of course if the hydrogen phosphate species nucleates first, the opposite logic applies until the phosphate compounds nucleate, but this would require two separate phosphate compounds to reach supersaturation and nucleate, which seems less probable. As growth proceeds, the trajectory of the pH will be determined by the relative sequestering of either or both phosphate or hydrogen phosphate in the solid phases.

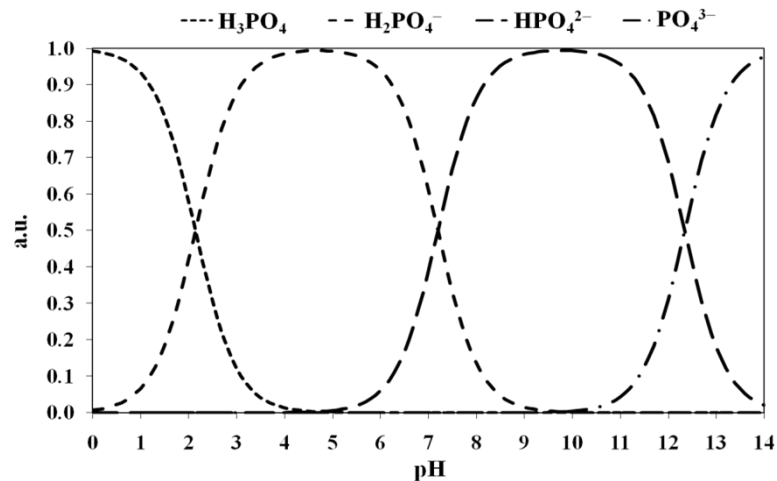


Fig. 7. pH variation of ionic concentrations in the triprotic equilibrium for phosphoric acid solutions.

At the beginning of the experiment, the pH gradient in the pure gel layer is predisposed to higher pH by the procedure of placing the pure gel solution on the phosphate gel layer. Diffusion of ions from the phosphate layer will commence immediately, and a small amount of the phosphate gel will dissolve before the “pure” gel sets. Both effects favor increased  $\text{PO}_4^{3-}$  ion concentration near the lead solution, favouring initial precipitation of the phosphate phases in the pure gel layer. The presence of PbHAp in the pure gel layer but not in the phosphate layer can be understood based on the higher  $\text{Pb}^{2+}:\text{PO}_4^{3-}$  ratio (5:3 vs. 3:2) required for the PbHAp phase relative to the  $\text{Pb}_3(\text{PO}_4)_2$  phase.

#### 4. Conclusion

Speciation calculations indicate the possibility of forming mixed phases of  $\text{PbHPO}_4$ ,  $\text{Pb}_3(\text{PO}_4)_2$ , and PbHAp in this system. XRD results confirm their formation, including the previously unreported gel precipitation of PbHAp. IR spectra of the crystalline products exhibit  $\nu_1$  and  $\nu_2$  vibrational bands indicating the lower point symmetry of  $\text{PO}_4^{3-}$  than tetrahedral. Formation of the microscopic crystalline products was accompanied by a decrease in pH from 8 (theoretical for all layers mixed) to 3 for all reactions studied, consistent with  $\text{PbHPO}_4$  being the major product. Formation of  $\text{PbHPO}_4$ ,  $\text{Pb}_3(\text{PO}_4)_2$ , and PbHAp phases with changing pH may be an important key for better understanding of the precipitation of biological hard tissues and the environmental geology of lead and phosphorus.

#### Acknowledgement

This research was supported by the Thai Commission on Higher Education (CHE) with a Ph.D. scholarship to OS.

#### References

- [1] T. K. Anee, M. Palanichamy, M. Ashok, N. M. Sundaram, and S. N. Kalkura, “Influence of iron and temperature on the crystallization of calcium phosphates at the physiological pH,” *Mater. Lett.*, vol. 58, pp. 478-482, 2004.
- [2] E. Ramachandran and S. Natarajan, “Crystal growth of some urinary stone constituents: II. In-vitro crystallization of hippuric acid,” *Cryst. Res. Technol.*, vol. 37, pp. 1274-1279, 2002.
- [3] E. K. Girija, Y. Yokogawa, and F. Nagata, “Apatite formation on collagen fibrils in the presence of polyacrylic acid,” *J. Mater. Sci.: Mater. Med.*, vol. 15, pp. 593-599, 2004.
- [4] D. M. C. Guimaraes, “Ferroelastic Transformations in lead orthophosphate and its structure as a function of temperature,” *Acta Crystallogr. Sect. A*, vol. 35, pp. 108-114, 1979.
- [5] D. L. Decker, S. Petersen, and D. Debray, “Pressure-induced ferroelastic phase transition in  $\text{Pb}_3(\text{PO}_4)_2$ : A neutron-diffraction study,” *Phys. Rev. B: Condens. Matter*, vol. 19, pp. 3552-3555, 1979.

- [6] C. C. Desai and M. S. V. Ramana, "Nucleation density and electrolytic growth of lead hydrogen phosphate single crystals in silica gels," *J. Cryst. Growth*, vol. 102, pp. 191-196, 1990.
- [7] C. C. Desai and M. S. V. Ramana, "Growth and properties of ferroelectric lead hydrogen phosphate and lead nitrate phosphate single crystals," *J. Cryst. Growth*, vol. 91, pp. 126-134, 1998.
- [8] M. C. Robert and F. Lefaucheux, "A comparative study of gel grown and space grown lead hydrogen phosphate crystals," *J. Cryst. Growth*, vol. 88, pp. 499-510, 1988.
- [9] B. Březina, M. Havránková, and K. Dušek, "The growth of  $\text{PbHPO}_4$  and  $\text{Pb}_4(\text{NO}_3)_2(\text{PO}_4)_2 \cdot 2\text{H}_2\text{O}$  in gels," *J. Cryst. Growth*, vol. 34, pp. 248-252, 1976.
- [10] R. Z. LeGeros, "Calcium phosphates in enamel, dentin, and bone," in *Calcium Phosphates in Oral Biology and Medicine*, 1st ed. San Francisco, USA: Karger, 1991, ch. 6, pp. 110-111.
- [11] D. L. Parkhurst and C. A. J. Appelo, *User's Guide to PHREEQC (version 2)-A Computer Program for Speciation, Batch-Reaction, One-Dimensional Transport, and Inverse Geochemical Calculations*. Denver, CO: U.S. Department of the Interior and U.S. Geological Survey, 1999.
- [12] E. Mavropoulos, C. C. N. Rocha, C. J. Moreira, M. A. Rossi, and A. G. Soares, "Characterization of phase evolution during lead immobilization by synthetic hydroxyapatite," *Mater. Charact.*, vol. 53, pp. 71-78, 2004.
- [13] V. M. Bhatnagar, "The preparation, x-ray and infrared spectra of lead apatites," *Archs. Oral Biol.*, vol.15, pp. 469-480, 1970.
- [14] R. Ternane, M. Ferid, M. Trabelsi-Ayedi, and B. Piriou, "Vibrational spectra of lead alkali apatites  $\text{Pb}_8\text{M}_2(\text{PO}_4)_6$  with  $\text{M} = \text{Ag}$  and  $\text{Na}$ ," *Spectrochim. Acta, Part A*, vol. 55, pp. 1793-1797, 1999.
- [15] A. A. Stepuk, A. G. Veresov, V. I. Putlyaev, and Yu. D. Tret'yakov, "The influence of  $\text{NO}_3^-$ ,  $\text{CH}_3\text{COO}^-$ , and  $\text{Cl}^-$  ions on the morphology of calcium hydroxyapatite crystals," *Dokl. Akad. Nauk*, vol. 412, pp. 11-14, 2007.
- [16] A. M. Ure and C. M. Davidson, "Predicting chemical speciation and computer simulation," in *Chemical Speciation in the Environment*, 1st ed. Glasgow, UK: Chapman and Hall, 1995, ch. 5, pp. 87-94.
- [17] W. Stumm and J. J. Morgan, "The equilibrium constant," in *Aquatic Chemistry*, 3rd ed. New York, NY: John Wiley & Sons, 1996, ch. 2, pp. 41-43.